First-Principles Study of Carbon and Vacancy Structures in Niobium

ARTICLE *in* THE JOURNAL OF PHYSICAL CHEMISTRY C · APRIL 2015

Impact Factor: 4.77 · DOI: 10.1021/acs.jpcc.5b00372

3 AUTHORS, INCLUDING:

Peter Zapol

Argonne National Laboratory

138 PUBLICATIONS **4,068** CITATIONS

SEE PROFILE

L. D. Cooley

Fermi National Accelerator Laboratory (Fermil…

137 PUBLICATIONS **2,649** CITATIONS

SEE PROFILE

THE JOURNAL OF PHYSICAL CHEMISTRY C

Article

pubs.acs.org/JPCC

First-Principles Study of Carbon and Vacancy Structures in Niobium

Denise C. Ford,[†] Peter Zapol,[†] and Lance D. Cooley*[,‡]

[†]Materials Science Division, Argonne National Laboratory, 9700 South Cass Avenue, Argonne, Illinois 60439, United States

[‡]Technical Division, Fermi National Accelerator Laboratory, Mail Stop 315, PO Box 500, Batavia, Illinois 60510 United States

ABSTRACT: The interstitial chemical impurities hydrogen, oxygen, nitrogen, and carbon are important for niobium metal production and particularly for the optimization of niobium SRF technology. These atoms are present in refined sheets and can be absorbed into niobium during processing treatments, resulting in changes to the residual resistance and the performance of SRF cavities. A first-principles approach is taken to study the properties of carbon in niobium, and the results are compared and contrasted with the properties of the other interstitial impurities. The results indicate that C will likely form precipitates or atmospheres around defects rather than strongly bound complexes with other impurities. On the basis of the analysis of carbon and hydrogen near niobium lattice vacancies and small vacancy chains and clusters, the formation of extended carbon chains and hydrocarbons is not likely to occur. Association of carbon with hydrogen atoms can, however, occur through the strain fields created by interstitial binding of the impurity atoms. Calculated electronic densities of states indicate that interstitial C may have a similar effect as interstitial O on the superconducting transition temperature of Nb.

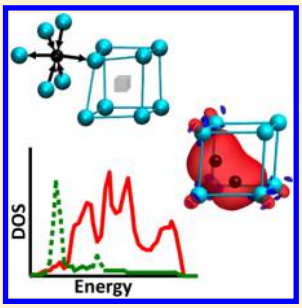

1. INTRODUCTION

Pure niobium is a primary material for superconducting technology, including superconducting radio frequency (SRF) cavities, superconducting electronic devices, and superconducting magnet strands and cables. Manufacturing activities generally strive to reduce the content of interstitial impurities H, O, N, and C to low levels because they degrade the superconducting properties, increase electron scattering, and increase the hardening rate during metal working. Interstitial oxygen, for example, reduces the superconducting transition temperature (T_c) by ~0.9 K per at %, and interstitial N and C are expected to have similar effects.[1] Especially, high purity, < 30 ppm by mass of O, N, and C and <5 ppm by mass H, is specified for Nb grades used in SRF cavities[2] to achieve high thermal conductivity at ~2 K.

Quite a bit of attention has been paid to the elements O and H in niobium, long ago due to applications of the metal in corrosive environments and in the presence of superheated steam[3] and more recently because etching and polishing of Nb with aqueous solutions has been used to remove defects introduced during the fabrication of SRF cavities.[4] Niobium forms a complex layering of oxides, including a diffusion gradient of interstitial oxygen, when the clean metal is exposed to air or water. The oxide is a good barrier against hydrogen at room temperature, but the structure and composition of the oxide layers changes upon heating to temperatures as low as 100 °C due to dissolution of oxygen into the metal.[5,6] Niobium absorbs copious amounts of hydrogen during electropolishing,[7] in conjunction with the electrochemical stripping of the oxides and the injection of vacancies to form an abundance of vacancy-hydrogen clusters.[8−10] If the hydrogen is not subsequently removed by annealing in high vacuum, niobium hydride precipitates can form at low temperature, leading to a sharp decrease in the cavity quality factor Q at the onset of RF field.[11] Even when hydrogen is degassed by annealing steps, small precipitates can still form,[12] leading to losses at high RF fields. Previously we analyzed how single H atoms may be trapped by single O or N atoms to prevent hydride phase formation.[13]

Interstitial N has received vigorous attention very recently, due to the apparent suppression of residual resistance at low RF field and the appearance of a field-dependent BCS residual resistance component.[14] The new behavior results in an increase in the cavity Q up to moderate fields, and it implies a factor-of-2 reduction in cryogenic operation cost. Because the introduction of N at high temperature is followed by a brief electropolishing to remove traces of surface nitrides, it might be possible that the remaining solid solution of N in Nb completely immobilizes H impurities, with N being more effective than O at trapping H, although this would not explain the unusual physics being reported. Two theoretical models have been presented[15,16] to explain the unusual surface resistance, where ref 16 pointed out that the addition of N may be crucial for changing Nb from clean-limit to dirty-limit regimes of BCS residual resistance in the presence of current flow. Besides nitrogen, titanium, which substitutes for Nb lattice sites and does not occupy interstitial lattice sites, has been shown to yield the new SRF cavity behavior.[17]

Although interstitial carbon in niobium has some similar properties to interstitial oxygen and nitrogen,[13] it has not been studied as intensively, perhaps because it has a much lower solubility.[18,19] The lack of attention paid to carbon in niobium may be an important oversight, however. Recent secondary ion

Special Issue: Steven J. Sibener Festschrift

Received: January 13, 2015
Revised: April 1, 2015

DOI: 10.1021/acs.jpcc.5b00372
J. Phys. Chem. C XXXX, XXX, XXX−XXX

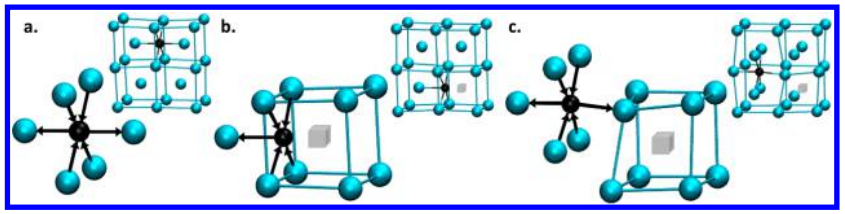

Figure 1. Configurations of one carbon atom in (a) an octahedral lattice interstice in bcc niobium, (b) an interior vacancy binding site, and (c) an exterior vacancy binding site. The insets show the configurations in a larger section of the Nb lattice. Niobium atoms are represented as blue spheres, carbon atoms as small black spheres, and niobium lattice vacancies as gray cubes. Black arrows indicate the direction of relaxation of Nb atoms upon absorption of a C atom into the binding site.

mass spectroscopy measurements of SRF niobium samples indicate local carbon concentrations of 10^{-1} to 10^{-2} at % depending on the specimen history and heat treatment,[17] and recent Raman spectroscopy studies indicate that large amounts of carbon are present in various forms as local clusters on niobium cavity and sample surfaces.[20] How the carbon collects is not known; the previously described reports emphasize clean handling and rule out casual environmental contributions. Dislocations seem to play a role because material working coupled to chemical polishing and annealing is a reproducible pathway toward the previously described results. Some carbide precipitates exhibit enhanced superconducting gaps, and Raman signatures suggested extremely strong electron−phonon coupling.[21] How different carbon configurations affect electronic and phonon properties is of interest to understand superconducting properties of technological Nb materials.

The superconducting properties of bulk niobium carbides and carbo-nitrides have been studied extensively in the past, as they present an interesting theoretical case study of electron−phonon superconductivity that is strongly dependent on composition and structure. The T_c of NbC has been shown to decrease with increasing concentration of carbon vacancies[22] and increase with the substitution of carbon for nitrogen.[23,24] NbN and NbC are very difficult to make at the stoichiometric ratio, which might reflect on structural instabilities at the root of superconductive electron pairing. Additionally, NbC_{1-x} up to $x \approx 0.25$ with disordered carbon vacancies has been shown to have a lower T_c than the ordered compound at a comparable concentration.[25]

In addition to carbon or carbide clusters in Nb and the bulk niobium carbide phases, the interaction of C with Nb is itself an interesting physical and metallurgical question. NbC precipitates are tremendously important to high-strength corrosion-resistant steels because the compound remains stable in austenitic stainless steels at high temperatures and the strain fields associated with NbC nanoprecipitates act as effective dislocation pinners.[26,27]

In the Nb−C system, C atoms might not necessarily precipitate as intermetallic phases or remain dissolved as a solid solution, but instead they can form atmospheres around lattice defects such as metal lattice vacancies, dislocations, or grain boundaries. C may be unique among the interstitial impurities by having a tendency to form dimers or chains, as C−C dimers in metal vacancies have been predicted for bcc Fe.[28−30] The formation of carbon clusters around dislocations has been observed as early as the 1960s,[31,32] and the migration of carbon atoms to grain boundaries upon heat treatment has recently been observed in SRF niobium.[33] Study of the interactions of carbon impurities with other defects can have a major effect on understanding the kinetic mechanisms in Nb processing.

In this study, we examine potential structures of carbon impurity and metal vacancy complexes in bcc niobium. Density functional theory (DFT) is used to compute the total energies and electronic structures of carbon atoms in bcc niobium interstitial sites, carbon atoms near niobium lattice vacancies, divacancies, and trivacancies, and several niobium carbides. The C−H interaction in niobium is also investigated. The results are discussed in terms of thermodynamic stability and electronic properties.

2. METHODS

Most of the impurity structures were modeled in a 4 × 4 × 4 unit cell of bcc niobium (128 atoms) with Nb atoms removed to create lattice vacancies, and C atoms were added in interstitial or vacancy binding sites. Some of the larger defect configurations required the use of 5 × 5 × 5 unit cells. The unit cells were chosen to be computationally efficient while minimizing interactions between periodic images. They are not intended to represent a specific concentration of defects. Several tests were performed for larger unit cells, and the conclusions drawn in this paper were upheld. Nb_2C was modeled in the β-LT structure, which has hexagonal symmetry and contains four formula units per unit cell, and NbC was modeled in the rock-salt structure with four formula units per unit cell.

All calculations were performed with the Vienna ab initio simulation package (VASP)[34,35] using DFT, periodic boundary conditions, and a plane-wave basis set with a 400 eV kinetic energy cutoff. The generalized gradient approximation (GGA) was used with the Perdew, Burke, Ernzerhof (PBE) exchange−correlation functional,[36] and the core electrons were described by the projector-augmented-wave (PAW) pseudopotentials.[37,38] All of the structure optimizations were calculated with all of the atom and cell degrees of freedom relaxed. Forces were converged to 0.02 eV/A. K points were selected by the Monkhorst−Pack[39] scheme with 2 × 2 × 2 gamma-centered grids for the geometry optimizations of the defect structures in niobium, 3 × 10 × 6 gamma-centered for Nb_2C, and 9 × 9 × 9 for NbC. Denser grids were used for the electronic densities of states (DOS) calculations: 6 × 6 × 6 gamma-centered grids for Nb defects, 5 × 19 × 12 gamma-centered for Nb_2C, and 13 × 13 × 13 for NbC. The partial occupancies for the one-electron levels were determined by the first-order Methfessel−Paxton method with a smearing width of 0.2 eV for the geometry optimizations, while the tetrahedron method with Blöchl corrections was used for the DOS calculations. Spin-polarization was not used for the calculations, after a check for selected configurations resulted in zero magnetic moment. The optimized lattice parameters for Nb, Nb_2C, and NbC are within 1% of their experimentally determined values.[40−42]

DOI: 10.1021/acs.jpcc.5b00372
J. Phys. Chem. C XXXX, XXX, XXX−XXX

Table 1. Elemental Data for Nb, C, N, O, and H; Interstitial Site Preference, Charge on the Interstitial Atom in the Nb Lattice, and Binding Energy (B.E.) for a C, N, O, and H Atom in a Nb Lattice Vacancy Referred to the Binding Energy for that Atom in its Preferred Interstitial Binding Site.[a]

	atomic radius (Å)[b]	Pauling electronegativity[c]	ground state electronic configuration	interstitial site preference[d]	charge on interstitial atom (e^-)[d]
Nb	1.45	1.60	[Kr] $4d^4$ $5s^1$	n.a.	n.a.
C	0.70	2.55	[He] $2s^2$ $2p^2$	octahedral	−1.76
N	0.65	3.04	[He] $2s^2$ $2p^3$	octahedral	−1.63
O	0.60	3.44	[He] $2s^2$ $2p^4$	octahedral	−1.35
H	0.25	2.20	$1s^1$	tetrahedral	−0.65
	B.E. (eV) for vacancy site b		charge on interstitial atom (e^-)	B.E. (eV) for vacancy site c	charge on interstitial atom (e^-)
C	0.00		−1.60	**−0.39**	−1.75
N	−0.25		−1.55	**−0.29**	−1.64
O	**−0.79**		−1.32	−0.22	−1.37
H	**−0.32**		−0.56	n.a.	n.a.

[a]Vacancy site b and vacancy site c are depicted in Figure 1b,c, respectively. The lowest energy is in bold, and n.a. stands for not applicable. [b]Ref 47. [c]Refs 48 and 49. [d]Ref 13.

Several energetic properties are discussed in the Results and Discussion section for comparison between structures. Binding energies were calculated from various reference states as were appropriate for the discussion, and these are specified in the Results and Discussion section. Negative (−) binding energies indicate that the bound state is lower in energy than the unbound state or reference state. Strain energies were calculated by subtracting the energy of the ideal bcc niobium lattice from the energy of the niobium lattice that was deformed from defects or impurities. In the cases of impurity absorption, the geometry was optimized with the impurity; then, the impurity was removed and a single-point energy calculation was done to determine the energy of the deformed lattice.

3. RESULTS AND DISCUSSION

Carbon impurity atoms occupy octahedral interstitial sites in bcc niobium. The binding configuration for a single carbon atom in Nb is shown in Figure 1a. As calculated previously in ref 13, absorption of carbon into the octahedral site imparts a large strain on the niobium lattice substantiated by a strain energy of 0.96 eV, a 25% expansion of the two "short" C−Nb bonds compared with what they would be in an undeformed octahedral site, and a 5% contraction of the four "long" C−Nb bonds. This indicates that C should preferentially bind to sites near structural lattice defects such as vacancies, dislocations, grain boundaries, interfaces, and surfaces; where the lattice strain imparted by the C atom can be reduced.

3.1. Interstitial Impurity Atoms near Single Lattice Vacancies. The calculated vacancy formation energy for niobium is 2.71 eV, which is in good agreement with the experimentally determined range 2.6 to 3.1 eV given in a review by Schultz and Ehrhart[43] and other first-principles calculations.[44,45] We explored several binding sites for a C atom near a single niobium lattice vacancy and show two configurations in Figure 1: the site preferred by H and O impurity atoms (ref 13 and refs therein) is depicted in Figure 1b and the site that we found to be the most energetically favorable for C is depicted in Figure 1c. The binding energies of C to the vacancy for these two configurations relative to C in an octahedral site far from a vacancy are 0.00 and −0.39 eV, respectively (Table 1). The niobium lattice strain energies for these two vacancy-binding configurations are 0.30 and 0.68 eV, respectively, which compares to the strain energy of 0.96 eV for C binding in an octahedral site far away from the vacancy. Although the reduction in strain energy is larger for C to migrate to a site where one of the short Nb−C bonds is eliminated (Figure 1b), C exhibits a strong preference for octahedral binding, maximizing the electronic interaction with Nb. This may be understood considering the elemental data provided in Table 1. The ground-state electron configuration of the C atom has four empty 2p states, resulting in the ability to form up to four covalent bonds in molecules. Carbon, however, does not form covalent bonds with Nb atoms in the bcc lattice, as can be seen in the charge density difference plots in Figure 2. Ionic nature

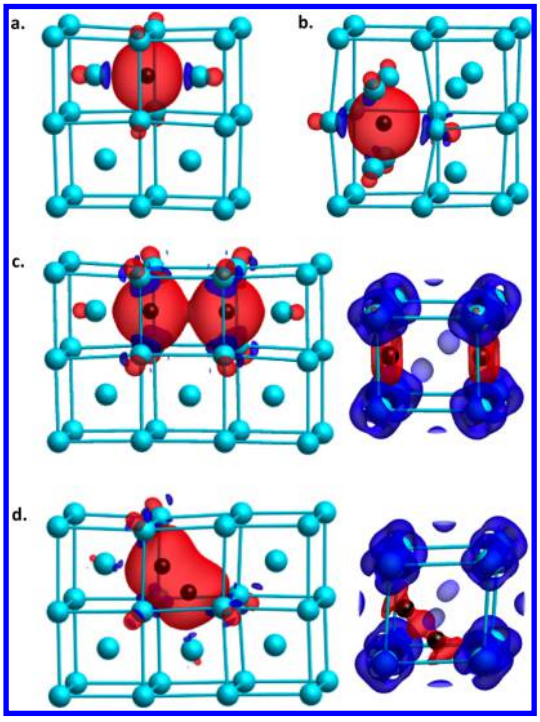

Figure 2. Charge density difference plots referred to the deformed niobium lattice with carbon atom(s) removed corresponding to the configurations in Figure 1a (a), Figure 1c (b), Figure 3a (c), and Figure 3b (d). The isosurface levels are 0.027 $e^-/Å^3$. The charge density difference referred to the overlapping atomic density is also shown for the configurations in panels c and d, with isosurface levels at 0.101 $e^-/Å^3$. Niobium atoms are represented as blue spheres and carbon atoms as small black spheres. The blue regions of charge density represent charge depletion and the red regions represent charge enhancement.

DOI: 10.1021/acs.jpcc.5b00372
J. Phys. Chem. C XXXX, XXX, XXX−XXX

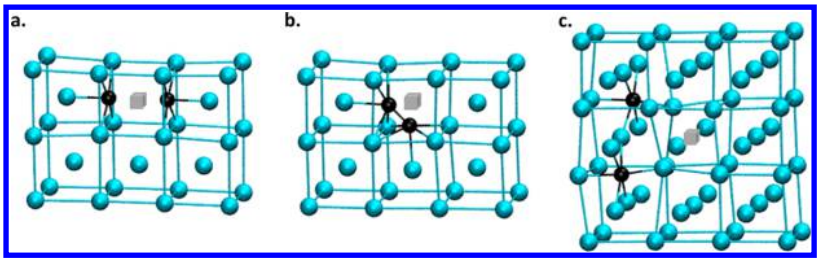

Figure 3. Configurations of two carbon atoms near a niobium lattice vacancy where they are in interior vacancy binding sites directly across from each other (a), offset from neighboring interior vacancy binding sites such that they form a dimer (b), and in the lowest energy exterior binding site configuration (c). Niobium atoms are represented as blue spheres, carbon atoms as small black spheres, and niobium lattice vacancies as gray cubes.

of bonding is observed, as indicated by the large region of electron density around the C atom, small regions of decreased electron density between the C and Nb atoms, and increased electron density near the Nb atoms in the opposite direction of the C atom. Carbon has a higher electronegativity than Nb, so it draws some of the Nb electrons onto itself, resulting in a partially anionic state. The charge on the carbon atom in the three binding configurations shown in Figure 1 was calculated with the Bader partitioning scheme[46] and is given in Table 1. The most favorable configuration for carbon near a Nb lattice vacancy allows for a greater charge on the carbon atom than does the less favorable configuration, even though the less favorable configuration provides more physical space for the C atom to occupy.

The basic elemental data, interstitial site preferences, vacancy binding energies, and charges in the bcc niobium lattice for a single H, O, and N atom are also reported in Table 1. Both interstitial and vacancy site preferences are correlated with the ground-state electronic configuration of the impurity atom and not with its size. H is s shell and prefers the sites in the Nb lattice with lower electron density (e.g., tetrahedral as opposed to octahedral interstitial sites). The other impurities are p shell and prefer the octahedral interstitial site. Their preference for binding near Nb vacancies (Figure 1b,c) depends on the number of 2p electrons in their ground-state electron configuration: more electrons in the p shell indicates a stronger preference for the configuration depicted in Figure 1b. H, O, and N are also more electronegative than Nb and therefore become partially anionic in the bcc niobium lattice, as previously discussed for C. The ability of each impurity atom to maintain its charge when binding near a vacancy correlates with its vacancy site preference. For example, O is able to maintain approximately the same charge in either of the vacancy binding sites considered as it had in an octahedral site far from the vacancy and therefore will bind in an interior vacancy site (Figure 1b) to minimize the lattice strain. However, C loses 0.16 e^- when binding in an interior binding site compared with an octahedral site far from the vacancy, whereas it maintains the same charge when binding in an exterior binding site close to the vacancy. N represents an intermediate case. The magnitude of charge on the impurity atoms is ordered as C > N > O > H, which follows the order of the atom sizes and the number of empty states in the atom's ground-state electron configuration rather than the electronegativity.

Figure 3 shows three possible configurations of two carbon atoms near a niobium lattice vacancy. We calculate a binding energy of −0.14 eV for two C atoms in interior octahedral binding sites that are directly across from each other (Figure 3a) relative to C atoms in octahedral interstitial sites far away from each other and any lattice vacancies. A C−C dimer with a bond length of 1.45 Å, which is in between the C−C single and double bond lengths, and a binding energy of −0.46 eV formed when two C atoms were placed in neighboring vacancy binding sites (Figure 3b). The electron density distributions for these two configurations are shown in Figure 2c,d, respectively. Small regions of reduced electron density between the Nb and C atoms grew when the isolevels were decreased below what is shown in the Figure, indicating that no covalent bonding occurs between the Nb and C atoms. Although it appears that the C atoms as shown in the first panel in Figure 2c may contain some overlapping electron density, no indication of covalent bonding was found between any of the atoms in this configuration when the overlapping atomic densities is taken as the reference (second panel). When the overlapping atomic densities is taken as the reference for the configuration appearing to contain a C−C dimer, an increased electron density between the two C atoms is apparent (second panel of Figure 2d), depicting the covalent nature of their bonding. The regions of reduced electron density surrounding the Nb atoms in both configurations, when the overlapping atomic densities is taken as the reference, indicates the metallic nature of the Nb bonding. The energetically most favorable configuration for two C atoms near a vacancy is neither of these configurations; however, it is instead where each C atom maintains an octahedral configuration within the Nb lattice and one of the short Nb−C bonds is with a Nb atom at the corner of the cube surrounding the vacancy (Figure 3c). This configuration allows the C atoms to maintain the maximum electronic interaction with the Nb atoms while reducing lattice strain, as previously discussed for the configurations of single carbon atoms near single lattice vacancies. The binding energy for this configuration is −0.89 eV. Note that this configuration is preferred to configurations where the C atoms are in octahedral binding sites near the vacancy and the short Nb−C bonds push the Nb atoms at the corners of the vacancy cube toward each other, which would cause repulsion between the Nb atoms, or both C atoms are bonded to the same vacancy-corner Nb, which would not provide sufficient electrons to the C atoms. The ability of niobium to accommodate C in vacancy binding sites as well as in the strain field around the vacancy suggests the possibility of Cottrell atmospheres[50] around these defect sites.

Carbon is unique among the interstitial impurity atoms, H, O, N, and C, in that it can form dimers in Nb lattice defects. We attempted to place pairs of interstitial atoms − H−H, O−O, N−N, and C−C − with gas phase dimer bond lengths in configurations similar to Figure 3b in a Nb lattice vacancy, as well as with one interstitial atom in an interior vacancy binding site and the other pointed toward the center of the vacancy. All

DOI: 10.1021/acs.jpcc.5b00372
J. Phys. Chem. C XXXX, XXX, XXX−XXX

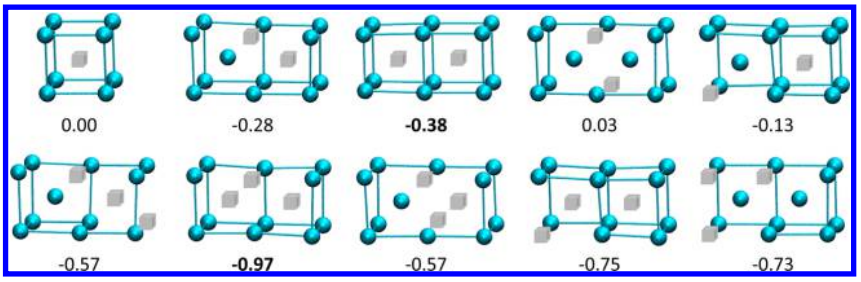

Figure 4. Configurations of niobium lattice defects and their interaction energies (in electronvolts) referred to single isolated vacancies. The formation energy of a single vacancy is 2.71 eV, and the lowest interaction energies for di- and tri-vacancies are in bold. Niobium atoms are represented as blue spheres and niobium lattice vacancies as gray cubes.

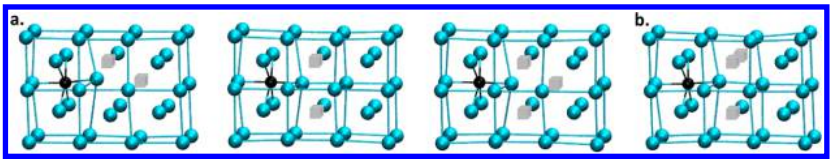

Figure 5. Configurations of a C atom near Nb di- and trivacancy clusters that have a lower binding energy than a C atom near a single Nb vacancy (a) and a configuration of C near a Nb trivacancy that has a similar binding energy to a C atom near a single Nb vacancy (b). Niobium atoms are represented as blue spheres, carbon atoms as small black spheres, and niobium lattice vacancies as gray cubes.

pairs except for C−C dissociated. This may be rationalized by considering the basic elemental data shown in Table 1. Carbon can form up to four covalent bonds to fill its 2p orbitals, so if it is in a position in the Nb lattice where it is facing a lower electron density, such as next to a Nb vacancy, it will form a covalent bond with an available neighboring carbon atom. The other p-block interstitial atoms considered here have more electrons in their 2p orbitals, therefore requiring less bonding electrons from their neighbors. C−C single bonds are stronger than N−N and O−O single bonds. Additionally, N and O have higher electronegativities than carbon, enabling them to more easily extract electrons from each neighboring Nb atom. H also has a higher electronegativity than Nb, therefore preferring to bond with Nb over another H atom.

3.2. Niobium Vacancy Dimer and Trimer Configurations and Their Interaction with Carbon Impurity Atoms. Optimized geometries for calculated configurations of niobium dimer and trimer vacancy clusters are shown in Figure 4. We find the second nearest-neighbor divacancy to be the most stable divacancy configuration, in agreement with previous experimental[51] and computational[52] studies, with a binding energy of −0.38 eV. The binding energy for vacancy trimers is approximately equal to the sum of the binding energies of vacancy pairs, and a triangle with two sides formed from pairs of nearest-neighbor divacancies and the third side formed from a pair of second-nearest neighbor divacancies is the most stable trivacancy configuration. Vacancies tend to migrate to sinks, such as surfaces, when they are mobile; however, if they find another vacancy or vacancy cluster first, they may become trapped. Reported vacancy migration energies range from 0.6 to 1.0 eV,[43,53] which is less than the 1.36 to 1.44 eV activation energy reported for C diffusion between octahedral interstitial sites.[54,55] Therefore, it is possible to form small vacancy clusters prior to vacancy trapping by C atoms. This conclusion would still apply in the cases where interstitial O, with an activation energy for diffusion of 1.17 eV,[55] or interstitial N, with an activation energy of 1.52 eV,[55] is present.

Additionally, vacancy dimers and linear trimers are reminiscent of edge dislocation cores, with the nearest-neighbor pair (chain) being in the [111] direction, the second-nearest neighbor pair (chain) being in the [100] direction, the third-nearest neighbor pair (chain) being in the [110] direction, and the fourth-nearest neighbor pair (chain) being in the [311] direction. Because the niobium atoms surrounding a vacancy relax toward the center of the vacancy, their Nb−Nb distances are shorter than in the bulk, so we speculate that the strain-field around a vacancy dimer (linear trimer) may be more representative of the compressive side of an edge dislocation than the expansive side. The nonlinear trimer configurations are similarly related to the lattice planes and therefore also to planar defects.

We calculated several binding configurations of carbon near first- and second-nearest neighbor divacancies and again found that configurations in which the carbon atom maintains full octahedral coordination with niobium atoms are more stable than configurations in which one of the niobium atoms is replaced by a vacancy. In some cases the binding energy for a C atom near a divacancy was more favorable than that for a C atom near a single vacancy because there is more space in the divacancy configuration for the Nb atom forming one of the short Nb−C bonds to be displaced. Examples of such a configuration for a first- and a second-nearest neighbor divacancy are shown in Figure 5. Both of these configurations have a binding energy of −0.49 eV, referred to a C atom in an octahedral site far away from the divacancy. Two configurations of C near a Nb trivacancy cluster are also shown in Figure 5. The configuration of C near the vacancy cluster in the (110) plane has a lower binding energy (−0.72 eV) than C near a single vacancy, whereas C near a (100) vacancy cluster has a comparable binding energy (−0.39 eV). The enthalpy of segregation to grain boundaries for C in Nb has been determined from the radio-tracer serial sectioning technique to be 49 kJ/mol,[56] which is in line with our calculation of multiple potential configurations of C near-planar defects with binding energies of that magnitude. Bokstein and Razumovskii[56] also measured C diffusion in niobium at 800−1173 K and report a lower activation energy and higher prefactor for grain boundary diffusion compared with bulk diffusion, which corroborates with our finding of weaker binding energies for

DOI: 10.1021/acs.jpcc.5b00372
J. Phys. Chem. C XXXX, XXX, XXX−XXX

the configurations with fewer C−Nb bonds in extended lattice defects than for the configurations with octahedrally coordinated C in the strain field around the lattice defects. Carbon diffusion is accelerated by ∼2 orders of magnitude in grain boundaries.[56,57]

C−C dimers are also more stable inside of a Nb nearest-neighbor divacancy than inside of a single vacancy. The configuration shown in Figure 6a, for example, has a binding

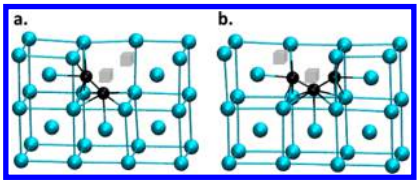

Figure 6. Configurations of a C−C dimer (a) and C_3 chain (b) near a nearest neighbor Nb divacancy. Niobium atoms are represented as blue spheres, carbon atoms as small black spheres, and niobium lattice vacancies as gray cubes.

energy of −0.60 eV, referred to isolated interstitial C atoms far from the divacancy. The binding energy reduces to −0.23 eV, however, when a trimer is formed (Figure 6b). Although we do not expect C chains to form in Nb defects, because the C−C dimer bond length is already longer than a double bond and the binding energy of a trimer in a divacancy is already reduced compared with the binding energy of a dimer, recent Raman spectroscopy measurements[20] indicate that we should consider the possibility more carefully. Therefore, we also selected two vacancy trimer configurations, the nearest-neighbor linear trimer and the lowest energy trimer cluster, to examine the possibility of forming chains of C atoms in extended Nb lattice defects. We found that a C_3 chain inside of a vacancy chain is less stable than C atoms in nearby octahedral sites around the vacancy chain (similar to Figure 1c). Inside of the vacancy cluster, configurations of a C−C dimer and a separate C were also more stable than the C_3 chain.

3.3. Comparison among Niobium Carbide Phases. The binding energies of selected configurations of carbon in niobium as well as the ordered niobium carbide phases are shown in Figure 7. Although the configurations of carbon near

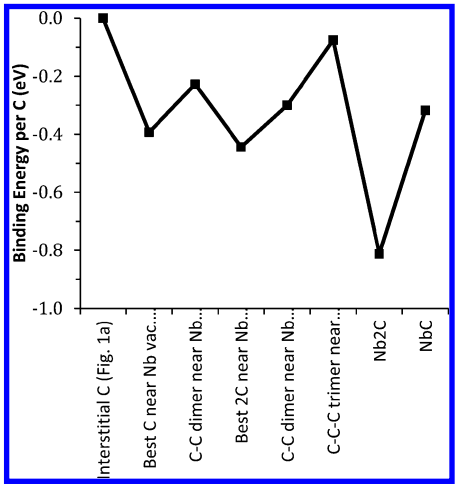

Figure 7. Binding energies of selected configurations of C in Nb relative to isolated C atoms in octahedral interstitial sites and niobium lattice vacancies or nearest-neighbor (NN) divacancies.

niobium lattice defects are favorable compared to interstitial carbon far away from lattice defects, Nb_2C has the lowest energy so will preferentially form under favorable kinetic conditions. Nb_2C has been formed in sputter-deposited thin films with compositions as low as 1.9% C.[19] Carbon has been shown to migrate to dislocations and replace oxygen in that region during strain aging experiments at 155 °C,[32] which may convert to carbide phases once a sufficient local concentration has been reached. Additional ordered phases that are not included in this study are present in experimental phase diagram,[18] and others have been predicted by first-principles calculations[58] as well.

3.4. Density of States and Trends in Superconductivity for NbC_x Systems. The C and Nb partial electronic DOS for pure Nb and interstitial C in Nb, Nb_2C, and NbC are shown in Figure 8, and corresponding DOS at the Fermi level (N_F) for these and selected other configurations of carbon in niobium are given in Table 2. The metallic band of pure bcc Nb in Figure 8 is ∼9 eV wide with a peak at the Fermi level. As C is added to the octahedral interstitial sites in Nb, C 2p states appear around −5 eV and these electrons bind to the Nb 5s electrons; this lowers N_F. Although N_F is not clearly correlated with T_c because it has both a direct proportionality and an indirect effect on the log-mean phonon frequency,[59] Koch et al.[60] has studied the Nb interstitial O system with a variety of experimental techniques and showed that the superconducting transition temperature, N_F, and electron−phonon coupling constant decrease with increasing oxygen concentration. Additionally, Dynes and Varma analyzed data for a number of transition metal alloys, including Nb−O, and concluded that the electron−phonon coupling parameter varies linearly with N_F.[61] We calculate a similar drop-off of N_F for interstitial C in Nb as Koch et al. report for interstitial O in Nb and show in ref 13 that interstitial C deforms the Nb lattice is a similar way as O but to a larger extent. Therefore, we predict a similar effect of interstitial C on niobium superconductivity as interstitial O imparts. Collection of carbon atoms around niobium vacancy-type defects, however, mitigates this effect (Table 2), as the portion of the effect due to lattice deformation is reduced.

As shown in Figure 8, the electronic structure of the niobium carbide alloy changes considerably as the carbon content increases and the crystal structure of the Nb lattice changes from bcc. The rock-salt structure of NbC has a lower N_F (Table 2) than Nb but a higher T_c. DFT calculations of the Fermi surface of NbC show that it contains nesting features that enhance the electron−phonon coupling.[62] The DOS for Nb_2C is intermediate in appearance between Nb with interstitial C and NbC, with strong overlap between the Nb and C states below −3 eV and mostly Nb states above. N_F is lower for Nb_2C than for Nb and NbC. Therefore, we suggest that T_c for Nb_2C is likely less than that for Nb or NbC.

3.5. Interaction Between Carbon and Hydrogen in the Niobium Lattice. Next, we calculate formation energies and structures of possible C−H complexes from C and H impurities in bcc Nb. We considered a C−H dimer inside of a single niobium vacancy and found that while it is stable, is less favorable by 0.20 eV compared with isolated interstitial C and H atoms far away from the vacancy. We also considered simple hydrocarbons C_3H_8, C_3H_5, and C_3H_2 in a chain of second nearest-neighbor Nb lattice vacancies, and in all cases the H atoms spontaneously dissociated from the C atoms during geometry optimization.

DOI: 10.1021/acs.jpcc.5b00372
J. Phys. Chem. C XXXX, XXX, XXX−XXX

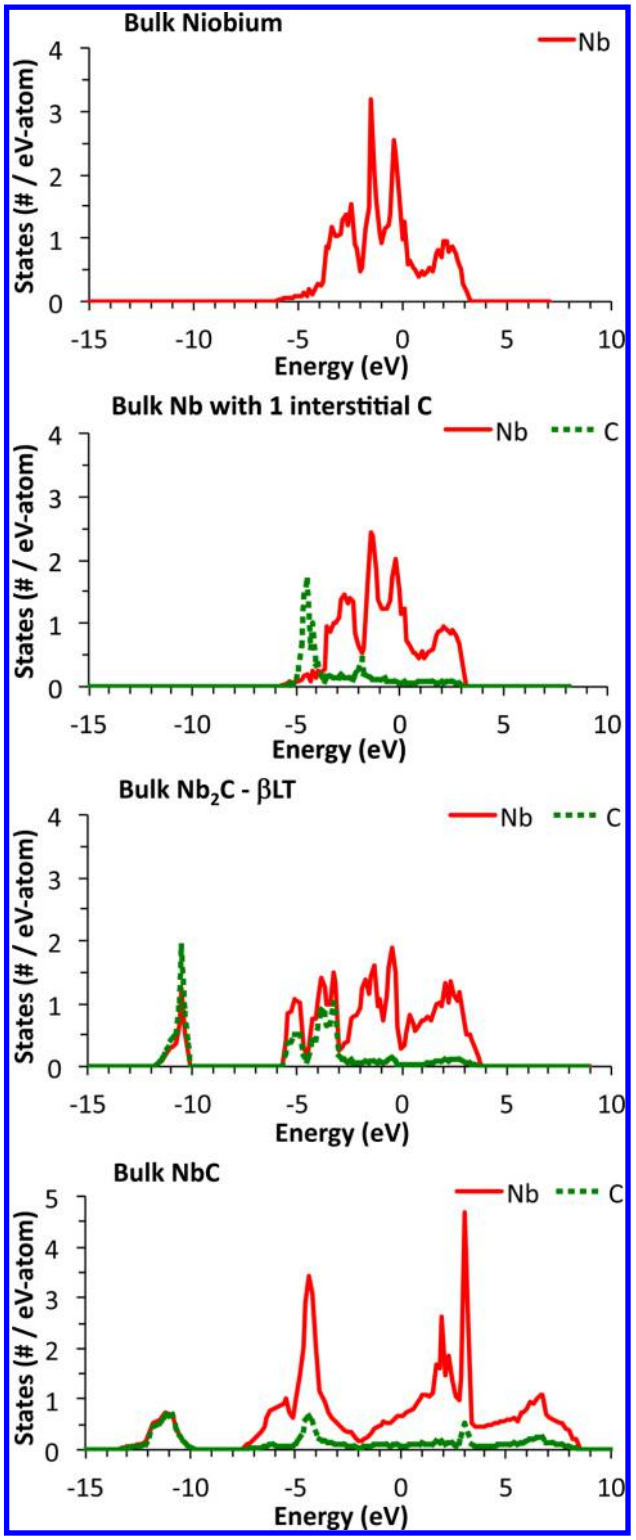

Figure 8. Partial electronic DOS of selected configurations of carbon in niobium, plotted with the Fermi energy at 0 eV.

Interstitial carbon atoms may, however, serve as trapping centers for interstitial hydrogen atoms. We calculated the binding energy for an H atom in a tetrahedral interstitial site 2−8.5 Å away from a C atom in an octahedral site and show the results in Figure 9 compared with the profiles for H trapping by O and N. All three profiles are similar, and the trapping energy is slightly greater for C and N than for O. The configuration for the lowest energy (C,N,O)−H pair is also shown in Figure 9. The C atom shares one bonding Nb atom with the H atom, and this Nb atom is displaced in the same direction, resulting from its interaction with the C atom and the H atom.

Table 2. DOS at the Fermi Level (N_F) for Selected Configurations of C in Nb

	N_F (no./eV atom)
Nb	1.53
Nb with 0.78% vacancies	1.51
Nb with 1.56% vacancies as nearest-neighbor divacancies	1.64
Nb with 0.78% C in octahedral sites	1.37
Nb with single C atoms near single vacancies (0.78%)	1.47
Nb with 1.56% C as two atoms near single vacancies	1.43
Nb with 1.56% C as dimers near vacancies	1.40
Nb_2C	0.21
NbC	0.38

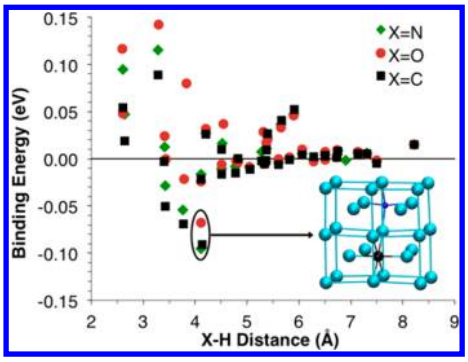

Figure 9. Plot of binding energy, referred to an H atom in a Nb tetrahedral interstitial site and a C, N, or O atom in an infinitely far away octahedral interstitial site versus the distance between a C, N, or O atom in an octahedral site and an H atom in a nearby tetrahedral site. The O data series was previously published in ref 13. The highest-energy configuration has a distance between the atoms of <2.5 Å and is not shown on the plot. An excerpt of lowest energy configuration is also shown; Nb atoms are represented as blue spheres, the C, N, or O is a small black sphere, and the H is a small dark-blue sphere.

4. CONCLUSIONS

First-principles calculations of carbon in Nb and its interactions with Nb vacancy-type defects, other C atoms, and H atoms show that C is likely to form precipitates or atmospheres around the vacancy-type defects rather than strongly bound complexes with other impurities. While Nb_2C is calculated to be the most stable phase for C in Nb, carbon-vacancy complexes can form stable states, which are competitive with NbC and may be favored kinetically in Nb processing. These are likely to be carbon atoms in octahedral interstitial positions near vacancies or extended lattice defects.

Carbon is unique among the interstitial impurities, H, O, N, and C, in that it can form dimers inside of Nb lattice vacancies. Extended chains of carbon atoms and hydrocarbon inclusions, however, do not seem to be favorable. Association of H with C atoms does occur in niobium through the strain field created by binding in interstitial sites, but a C−H bond does not form.

The electronic DOS at the Fermi level decreases for interstitial C, similar to interstitial O, indicating that a similar decrease in T_c may follow. Binding of C near lattice defects somewhat mitigates this effect.

DOI: 10.1021/acs.jpcc.5b00372
J. Phys. Chem. C XXXX, XXX, XXX−XXX

AUTHOR INFORMATION

Corresponding Author

*E-mail: ldcooley@fnal.gov. Tel: 630-840-6797.

Notes

The authors declare no competing financial interest.

ACKNOWLEDGMENTS

We acknowledge computer resources from Fermilab, Argonne LCRC, and Argonne Center for Nanoscale Materials. Argonne National Laboratory, a U.S. Department of Energy Office of Science laboratory, is operated under contract no. DE-AC02-06CH11357.

REFERENCES

(1) DeSorbo, W. Effect of Dissolved Gases on Some Superconducting Properties of Niobium. *Phys. Rev.* **1963**, *132*, 107−121.

(2) Cooley, L. Technical Specifications for High RRR Grade Niobium Sheet for Use in Superconducting Radio Frequency Cavities Fermilab Specification 5500.000-ES-371037, 2011.

(3) Bauer, A. A.; Berry, W. E.; DeMastry, J. A.; Koester, R. D.; Rough, F. A. *Development of Niobium Alloys Resistant to Superheated Steam*; Battelle Memorial Institute: Columbus, 1964.

(4) Padamsee, H. *RF Superconductivity Science,Technology and Applications*; Wiley-VCH: Weinheim, Germany, 2009; Vol. 2.

(5) Ma, Q.; Ryan, P.; Freeland, J. W.; Rosenberg, R. A. Thermal Effect on the Oxides on Nb(100) Studied by Synchrotron-Radiation X-Ray Photoelectron Spectroscopy. *J. Appl. Phys.* **2004**, *96*, 7675−7680.

(6) Delheusy, M.; Stierle, A.; Kasper, N.; Kurta, R. P.; Vlad, A.; Dosch, H.; Antoine, C.; Resta, A.; Lundgren, E.; Andersen, J. X-Ray Investigation of Subsurface Interstitial Oxygen at Nb/Oxide Interfaces. *Appl. Phys. Lett.* **2008**, *92*, 101911.

(7) Ricker, R. E.; Myneni, G. R. Evaluation of the Propensity of Niobium to Absorb Hydrogen During Fabrication of Superconducting Radio Frequency Cavities for Particle Accelerators. *J. Res. Natl. Inst. Stand. Technol.* **2010**, *115*, 353−371.

(8) Fukai, Y.; Okuma, N. Evidence of Copious Vacancy Formation in Ni and Pd under a High Hydrogen Pressure. *Jpn. J. Appl. Phys.* **1993**, *32*, L1256−L1259.

(9) Fukai, Y.; Okuma, N. Formation of Superabundant Vacancies in Pd Hydride under High Hydrogen Pressures. *Phys. Rev. Lett.* **1994**, *73*, 1640−1643.

(10) Koike, H.; Shizuku, Y.; Yazaki, A.; Fukai, Y. Superabundant Vacancy Formation in Nb−H Alloys; Resistometric Studies. *J. Phys.: Condens. Matter* **2004**, *16*, 1335−1349.

(11) Knobloch, J. The "Q Disease" in Superconducting Niobium RF Cavities. In *First International Workshop on Hydrogen in Materials and Vacuum Systems*; Myneni, G. R., Chattopadhyay, S., Eds.; AIP: Melville, NY, 2003; pp 133−150.

(12) Ciovati, G.; Myneni, G.; Stevie, F.; Maheshwari, P.; Griffis, D. High Field Q Slope and the Baking Effect: Review of Recent Experimental Results and New Data on Nb Heat Treatments. *Phys. Rev. Spec. Top.–Accel. Beams* **2010**, *13*, 022002.

(13) Ford, D. C.; Cooley, L. D.; Seidman, D. N. Suppression of Hydride Precipitates in Niobium Superconducting Radio-Frequency Cavities. *Supercond. Sci. Technol.* **2013**, *26*, 105003.

(14) Grassellino, A.; Romanenko, A.; Sergatskov, D.; Melnychuk, O.; Trenikhina, Y.; Crawford, A.; Rowe, A.; Wong, M.; Khabiboulline, T.; Barkov, F. Nitrogen and Argon Doping of Niobium for Superconducting Radio Frequency Cavities: A Pathway to Highly Efficient Accelerating Structures. *Supercond. Sci. Technol.* **2013**, *26*, 102001.

(15) Xiao, B. P.; Reece, C. E. A New First-Principles Calculation of Field-Dependent RF Surface Impedance of BCS Superconductor and Application to SRF Cavities. arXiv:1404.2523v1 [cond-mat.supr-con], 2014.

(16) Gurevich, A. Reduction of Dissipative Nonlinear Conductivity of Superconductors by Static and Microwave Magnetic Fields. *Phys. Rev. Lett.* **2014**, *113*, 087001.

(17) Dhakal, P.; et al. Effect of High Temperature Heat Treatments on the Quality Factor of a Large-Grain Superconducting Radio-Frequency Niobium Cavity. *Phys. Rev. Spec. Top.–Accel. Beams* **2013**, *16*, 042001.

(18) Huang, W. *C-Nb Phase Diagram*; ASM International: Materials Park, OH, 2006. http://www1.asminternational.org/AsmEnterprise/APD.

(19) Volodin, V. N.; Teleushev, Y. Z.; Zhakanbaev, E. A. Structure and Phase Composition of Nb−C Deposited Films. *Phys. Met.* **2013**, *114*, 395−399.

(20) Cao, C.; Ford, D.; Bishnoi, S.; Proslier, T.; Albee, B.; Hommerding, E.; Korczakowski, A.; Cooley, L.; Ciovati, G.; Zasadzinski, J. F. Detection of Surface Carbon and Hydrocarbons in Hot Spot Regions of Niobium Superconducting RF Cavities by Raman Spectroscopy. *Phys. Rev. Spec. Top.–Accel. Beams* **2013**, *16*, 064701.

(21) Cao, C.; et al. Giant Two-Phonon Raman Scattering from Nanoscale NbC Precipitates in Nb. *Phys. Rev. B* **2015**, *91*, 094302.

(22) Giorgi, A. L.; Szklarz, E. G.; Storms, E. K.; Bowman, A. L.; Matthias, B. T. Effect of Composition on the Superconducting Transition Temperature of Tantalum Carbide and Niobium Carbide. *Phys. Rev.* **1962**, *125*, 837−838.

(23) Toth, L. E. *Transition Metal Carbides and Nitrides*; Academic Press: New York, 1971.

(24) Blackburn, S.; Cote, M.; Louie, S.; Cohen, M. L. Enhanced Electron-Phonon Coupling near the Lattice Instability of Superconducting $NbC_{1-x}N_x$ from Density-Functional Calculations. *Phys. Rev. B* **2011**, *84*, 104506.

(25) Rempe, A. I. G. A. A. Superconductivity in Disordered and Ordered Niobium Carbide. *Phys. Status Solidi B* **1989**, *151*, 211−224.

(26) Shrestha, S. L.; Xie, K. Y.; Ringer, S. P.; Carpenter, K. R.; Smith, D. R.; Killmorec, C. R.; Cairneya, J. M. The Effect of Clustering on the Mobility of Dislocations During Aging in Nb-Microalloyed Strip Cast Steels: In Situ Heating TEM Observations. *Scr. Mater.* **2013**, *69*, 481−484.

(27) Dutta, B.; Palmiere, E. J.; Sellars, C. M. Modelling the Kinetics of Strain Induced Precipitation in Nb Microalloyed Steels. *Acta Mater.* **2001**, *49*, 785−794.

(28) Johnson, R. A.; Dienes, G. J.; Damask, A. C. Calculations of the Energy and Migration Characteristics of Carbon and Nitrogen in α-Iron and Vanadium. *Acta Metall.* **1964**, *12*, 1215−1224.

(29) Domain, C.; Becquart, C. S.; Foct, J. Ab Initio Study of Foreign Interstitial Atom (C, N) Interactions with Intrinsic Point Defects in α-Fe. *Phys. Rev. B* **2004**, *69*, 144112.

(30) Fu, C.-C.; Meslin, E.; Barbu, A.; Willaime, F.; Oison, V. Effect of C on Vacancy Migration in α-Iron. *Solid State Phenom.* **2008**, *139*, 157−164.

(31) Szkopiak, Z. C.; Derry, L. W. Some Strain-Ageing Effects in Commercial Niobium. *J. Nucl. Mater.* **1964**, *13*, 130−136.

(32) Szkopiak, Z. C.; Miodownik, A. P. The Mechanism of Strain-Ageing in Commercially Pure Niobium. *J. Nucl. Mater.* **1965**, *17*, 20−29.

(33) Maheshwari, P.; Zhou, C.; Stevie, F. A.; Myneni, G. R.; Spradlin, J.; Ciovati, G.; Rigsbee, J. M.; Batchelor, A. D.; Griffis, D. P. SIMS and TEM Analysis of Niobium Bicrystals. In *Proceedings of SRF2011*, Chicago, IL, 2011; p THPO028.

(34) Kresse, G.; Furthmuller, J. Efficient Iterative Schemes for Ab Initio Total-Energy Calculations Using a Plane-Wave Basis Set. *Phys. Rev. B* **1996**, *54*, 11169−11186.

(35) Kresse, G.; Hafner, J. Abinitio Molecular-Dynamics for Liquid-Metals. *Phys. Rev. B* **1993**, *47*, 558−561.

(36) Perdew, J. P.; Burke, K.; Ernzerhof, M. Generalized Gradient Approximation Made Simple. *Phys. Rev. Lett.* **1996**, *77*, 3865−3868.

(37) Kresse, G.; Joubert, D. From Ultrasoft Pseudopotentials to the Projector Augmented-Wave Method. *Phys. Rev. B* **1999**, *59*, 1758−1775.

DOI: 10.1021/acs.jpcc.5b00372
J. Phys. Chem. C XXXX, XXX, XXX−XXX

(38) Blochl, P. E. Projector Augmented-Wave Method. *Phys. Rev. B* **1994**, *50*, 17953−17979.
(39) Monkhorst, H. J.; Pack, J. D. Special Points for Brillouin-Zone Integrations. *Phys. Rev. B* **1976**, *13*, 5188−5192.
(40) Huber, K. P.; Herzberg, G. *Molecular Spectra and Molecular Structure. IV. Constants of Diatomic Molecules*; Van Nostrand Reinhold Co.: New York, 1979.
(41) Khaenko, B. V.; Gnitetskii, O. A. *Kristallografiya* **1993**, *38*, 741.
(42) Will, G.; Platzbecker, R. *Z. Anorg. Allg. Chem.* **2001**, *627*, 2207.
(43) Schultz, H.; Ehrhart, P. In *Atomic Defects in Metals*; Ullmaier, H., Ed.; Springer: Berlin, 1991; Vol. 25.
(44) Korhonen, T.; Puska, M. J.; Nieminen, R. M. Vacancy-Formation Energies for Fcc and Bcc Transition Metals. *Phys. Rev. B* **1995**, *51*, 9526−9532.
(45) Korzhavyi, P. A.; Abrikosov, I. A.; Johansson, B. First-Principles Calculations of the Vacancy Formation Energy in Transition and Noble Metals. *Phys. Rev. B* **1999**, *59*, 11693−11703.
(46) Henkelman, G.; Arnaldsson, A.; Jonsson, H. A Fast and Robust Algorithm for Bader Decomposition of Charge Density. *Comput. Mater. Sci.* **2006**, *36*, 354−360.
(47) Slater, J. C. Atomic Radii in Crystals. *J. Chem. Phys.* **1964**, *41*, 3199−3204.
(48) Allred, A. L. Electronegativity Values from Thermochemical Data. *J. Inorg. Nucl. Chem.* **1961**, *17*, 215−221.
(49) Pauling, L. *The Nature of the Chemical Bond*, 3rd ed.; Cornell Univ.: Ithaca, NY, 1960.
(50) Cottrell, A. H.; Bilby, B. A. Dislocation Theory of Yielding and Strain Ageing of Iron. *Proc. Phys. Soc., London, Sect. A* **1949**, *62*, 49−62.
(51) Metzner, H.; Sielemann, R.; Klaumtinzer, S.; Butt, R.; Semmler, W. Intrinsic Point Defects in Niobium: Trapping at ^{100}pd and ^{111}In Impurities Observed by PAC. *Z. Phys. B* **1985**, *61*, 267−281.
(52) Derlet, P. M.; Nguyen-Manh, D.; Dudarev, S. L. Multiscale Modeling of Crowdion and Vacancy Defects in Body-Centered-Cubic Transition Metals. *Phys. Rev. B* **2007**, *76*, 054107.
(53) Nguyen-Manh, D.; Horsfield, A. P.; Dudarev, S. L. Self-Interstitial Atom Defects in Bcc Transition Metals: Group-Specific Trends. *Phys. Rev. B* **2006**, *73*, 020101.
(54) Li, C.-X.; Luo, H.-B.; Hu, Q.-M.; Yin, F.-X.; Umezawa, O.; Yang, R. Theoretical Investigations of Interstitial Atoms in Bcc Metals: Local Lattice Distortion and Diffusion Barrier. *Comput. Mater. Sci.* **2012**, *58*, 67−70.
(55) Powers, R. W.; Doyle, M. V. Diffusion of Interstitial Solutes in the Group V Transition Metals. *J. Appl. Phys.* **1959**, *30*, 514−524.
(56) Bokstein, B.; Razumovskii, I. Grain Boundary Diffusion and Segregation in Interstitial Solid Solutions Based on Bcc Transition Metals: Carbon in Niobium. *Interface Sci.* **2003**, *11*, 41−49.
(57) Vasilenok, L. B.; Kablov, E. N.; Bokshtein, B. S.; Razumovskii, I. M. Diffusion of Carbon Along Grain Boundaries in Niobium. *Dokl. Phys.* **2000**, *45*, 588−591.
(58) Wu, L.; Wang, Y.; Yan, Z.; Zhang, J.; Xiao, F.; Liao, B. The Phase Stability and Mechanical Properties of Nb−C System: Using First-Principles Calculations and Nano-Indentation. *J. Alloys Compd.* **2013**, *561*, 220−227.
(59) Butler, W. H. Electron-Phonon Coupling in the Transition Metals: Electronic Aspects. *Phys. Rev. B* **1977**, *15*, 5267−5282.
(60) Koch, C. C.; Scarbrough, J. O.; Kroeger, D. M. Effects of Interstitial Oxygen on the Superconductivity of Niobium. *Phys. Rev. B* **1974**, *9*, 888−897.
(61) Dynes, R. C.; Varma, C. M. Superconductivity and Electronic Density of States. *J. Phys. F: Met. Phys.* **1976**, *6*, L215−L219.
(62) Isaev, E. I.; Simak, S. I.; Abrikosov, I. A.; Ahuja, R.; K.Vekilov, Y.; Katsnelson, M. I.; Lichtenstein, A. I.; Johansson, B. Phonon Related Properties of Transition Metals, Their Carbides, and Nitrides: A First-Principles Study. *J. Appl. Phys.* **2007**, *101*, 123519.

DOI: 10.1021/acs.jpcc.5b00372
J. Phys. Chem. C XXXX, XXX, XXX−XXX